HAL
open science

Boundary data reconstruction for open channel networks using modal decomposition

Q. Wu, X. Litrico, Aurélie Bayen-Poisson

To cite this version:

Q. Wu, X. Litrico, Aurélie Bayen-Poisson. Boundary data reconstruction for open channel networks using modal decomposition. 47th IEEE Conference on Decision and Control, Dec 2008, Cancun, Mexico. p. 3903 - p. 3910, 10.1109/CDC.2008.4739010 . hal-00468555

HAL Id: hal-00468555

https://hal.science/hal-00468555v1

Submitted on 31 Mar 2010

HAL is a multi-disciplinary open access archive for the deposit and dissemination of scientific research documents, whether they are published or not. The documents may come from teaching and research institutions in France or abroad, or from public or private research centers.

L'archive ouverte pluridisciplinaire **HAL**, est destinée au dépôt et à la diffusion de documents scientifiques de niveau recherche, publiés ou non, émanant des établissements d'enseignement et de recherche français ou étrangers, des laboratoires publics ou privés.

Open Channel Flow Estimation and Data Reconciliation using Modal Decomposition

Qingfang Wu*, Xavier Litrico† and Alexandre M. Bayen*
*Department of Civil and Environmental Engineering, UC Berkeley, CA, USA
{qingfangwu,bayen}@berkeley.edu
†Cemagref, UMR G-EAU, B.P. 5095, 34196 Montpellier Cedex 5, France
{xavier.litrico}@cemagref.fr

***Abstract*— This article presents a method to estimate flow variables for an open channel network governed by first-order, linear hyperbolic partial differential equations and subjected to periodic forcing. The selected external boundary conditions of the system are defined as the model input; the flow properties at internal locations, as well as the other external boundary conditions, are defined as the output. A spatially-dependent transfer matrix in the frequency domain is constructed to relate the model input and output. A data reconciliation technique efficiently eliminates the error in the measured data and results in a reconciliated external boundary conditions; subsequently, the flow properties at any location in the system can be accurately evaluated. The applicability and effectiveness of the method is substantiated with a case study of the river flow subject to tidal forcing in the Sacramento-San Joaquin Delta, California. It is shown that the proposed method gives an accurate estimation of the flow properties at any intermediate location within the channel network.**

I. Introduction

Hydrodynamic flows in complex networks subjected to tidal forcing have been widely explored in environmental engineering. A reliable characterization of flow properties in the network generally demands a complex nonlinear model, for example, *Delta Simulation Model II* (DSM2) [1], Shallow Water Equation (SWE) solver package *TELEMAC* [2], and the software *Mike21* developed by *Danish Hydraulic Institute* (DHI) Group [3]. Constructing and utilizing these state-of-the-art mathematical computer models is very important for decision support in operations, planning, and managing water supply and water quality.

However, the construction of such large-scale nonlinear models is usually a complex task. It requires detailed information of network geometry, as well as precise measurements at the boundaries, which is, unfortunately, often unavailable. Also, the resulting nonlinear models are constructed referring to a specific river channel, and hardly transferable to other networks.

For networks of open-channels, one-dimensional unsteady flow model can be used to simulate the flow. Numerous 1-D river hydraulics models are based on the Saint-Venant Equations, using either an implicit or explicit finite difference scheme [4] [5] or finite-element method [6]. The main advantage of these models is that they can be easily constructed by numerical simulations with standard schemes, and that they are suitable to any flow configurations. However, considering the system in a frequency domain leads to a linear model which is easier to simulate [7].

For channels in the uniform flow regime, in which the geometry is uniform and the water depth is constant along the channel, it is well known that an analytical solution to the *Linearized Saint-Venant equations* (LSVE) exists in the frequency domain [8] [9] [10]. However, realistic channels hardly exhibit uniform flows. To better represent realistic flow conditions, the backwater curve model is introduced [11]. A transfer matrix function corresponding to LSVE and characterizing the more realistic flow conditions has been presented [12].

The present article extends the transfer matrix function into a channel network. A spatially dependent transfer matrix is constructed, relating a selected set of model inputs to the output variables. This transfer matrix is a function of channel width, channel length, bed slope, mean discharge, mean stage and Manning coefficient, since set of parameter needs to be chosen carefully to characterize the geometry of the channel, since the uncertainty of the parameters contribute to the error in model output.

Another concern regarding the model accuracy is the validity of the measured data. Numerous factors could lead to measurement errors, for example, the limitation of instruments, the human errors, etc. It is imperative to minimize these measurement errors to improve the performance of our channel model. Static data reconciliation, as an effective method to tune-up the measurement data [13] [14] [15] [16], has been applied in several engineering fields [17] [18] [19]. In this article, we "reconstruct" the boundary conditions using static data reconciliation, and use them in the channel network model for an accurate simulation of the flow. As a result, we obtain a new set of boundary data which are consistent with the model and are consistent with statistical assumptions on measurement errors. Finally, we use this data to obtain the flow inside of the domain.

This paper is organized as follows, Section II introduces the LSWE in the frequency domain, along with the discussion of spatially-dependent transfer matrix. A channel network model featuring one-dimensional non-uniform flow is subsequently described. Section III presents the model to a channel network system in the Sacramento - San Joaquin Delta in California. Static data reconciliation is applied to eliminate the error in the measurements. The effectiveness of the model is verified by correlating the model estimations with the field

data at three intermediate locations in the network. Section IV summarizes the studies and presents the scope of our future work.

II. Channel Network Model

A. The Saint-Venant model

The Saint-Venant equations are quasi-linear hyperbolic *partial differential equations* (PDEs), which are widely used in open-channel hydraulic systems [20],[21]. For a rectangular cross-section, these equations are given by:

$$TY_t + Q_x = 0 \tag{1}$$

$$Q_t + \left(\frac{Q^2}{TY} + \frac{gTY^2}{2}\right)_x + gTY\left(S_f - S_b\right) = 0 \tag{2}$$

for $(x,t) \in (0,X) \times \Re^+$, where X is the river reach (m), $Q(x,t)$ is the discharge (m^3/s) across cross-section $A(x,t) = TY(x,t)$, $Y(x,t)$ is the stage (m), T is the free surface width (m) which is a constant for rectangular cross-section, g is the gravitational acceleration (m/s^2), S_b is the bed slope (m/m), $S_f(x,t)$ is the friction slope (m/m) modeled by Manning-Strickler's formula (3), with n is the Manning's roughness coefficient $(sm^{-1/3})$.

$$S_f = \frac{Q^2 n^2 (T+2Y)^{4/3}}{(TY)^{10/3}} \tag{3}$$

The boundary conditions for this system are discharge at upstream $Q(0,t) = Q_0(t)$ and stage at downstream $Y(X,t) = Y_X(t)$. The initial conditions are given by $Q(x,0)$ and $Y(x,0)$ for $x \in [0,X]$.

Equations (1,2) admit a *steady state solution* under constant boundary conditions. Let the flow variables corresponding to the steady state condition be denoted by $Q_0(x)$, $Y_0(x)$. where $x \in [0,X]$. The steady state equations are:

$$\frac{dQ_0(x)}{dx} = 0 \tag{4}$$

$$\frac{dY_0(x)}{dx} = \frac{S_b - S_{f0}}{1 - F_0(x)^2} \tag{5}$$

with $C_0 = \sqrt{gY_0}$ is the wave celerity, $F_0 = V_0/C_0$ is the Froude number and $V_0 = Q_0/A_0$ is the steady state velocity. While the first equation indicates $Q_0(x) = Q_0 = Q_X$, the second equation is solved for $Y_0(x)$ with boundary condition $Y_0(X)$. In this article, we assume the flow to be *sub-critical*, i.e., $F_0 < 1$.

B. Linearized Saint-Venant model

Equation (2) in the Saint-Venant model is nonlinear in the flow variables Q and Y. Each term $f(Q,Y)$ in the Saint-Venant model can be expanded into Taylor series around the steady state flow variables $Q_0(x)$ and $Y_0(x)$. Considering only the first-order perturbations, each term can be approximated as: $f(Q,Y) \approx f(Q_0,Y_0) + (f_Q)_0\, q(x,t) + (f_Y)_0\, y(x,t)$ where, the first order perturbations in discharge and stage are given by $q(x,t) = Q(x,t) - Q_0(x)$ and $y(x,t) = Y(x,t) - Y_0(x)$ respectively.

From [22], the linearized Saint-Venant model for the perturbed flow variables q and y reads:

$$T_0 y_t + q_x = 0 \tag{6}$$

$$q_t + 2V_0(x)q_x - \beta_0(x)q + \alpha_0(x)y_x - \gamma_0(x)y = 0 \tag{7}$$

where $\alpha_0(x)$, $\beta_0(x)$ and $\gamma_0(x)$ are given by:

$$\alpha_0 = (C_0^2 - V_0^2)T_0 \tag{8}$$

$$\beta_0 = -\frac{2g}{V_0}\left(S_b - \frac{dY_0}{dx}\right) \tag{9}$$

$$\gamma_0 = gT_0\left[(1+\kappa_0)S_b - (1+\kappa_0-(\kappa_0-2)F_0^2)\frac{dY_0}{dx}\right] \tag{10}$$

with $\kappa_0 = 7/3 - 8Y_0/(3(2Y_0+T))$. In the above equations, a uniform width at the free surface is assumed (denoted as T_0). The upstream and downstream boundary conditions are featured by the upstream discharge perturbation $q(0,t)$ and the downstream stage perturbation $y(X,t)$, respectively. The initial conditions are given by $y(x,0) = 0$ and $q(x,0) = 0$ for all $x \in [0,X]$.

The linearized Saint-Venant model (6,7) can also be written in the following form:

$$u_t = \mathcal{A}(x)u \tag{11}$$

where u is defined by the two-dimensional vector function as:

$$u(x,t) = \begin{pmatrix} u_1(x,t) \\ u_2(x,t) \end{pmatrix} := \begin{pmatrix} q(x,t) \\ y(x,t) \end{pmatrix}, \quad (x,t) \in \Re^+ \tag{12}$$

$\mathcal{A}(x)$ denotes the linear operator as:

$$\mathcal{A}(x) = \begin{pmatrix} 0 & \frac{1}{T_0} \\ \alpha_0(x) & 2V_0(x) \end{pmatrix}\frac{\partial}{\partial x} + \begin{pmatrix} 0 & 0 \\ \gamma_0(x) & \beta_0(x) \end{pmatrix} \tag{13}$$

The boundary conditions of (11) are:

$$u_1(0,t) \text{ and } u_2(X,t) \tag{14}$$

and initial conditions are:

$$u(x,0) = 0, \forall x \in [0,X] \tag{15}$$

C. Transfer matrix representation of Saint-Venant model for uniform flow case

The application of Laplace transform to the linear PDE system (11) leads to the *ordinary differential equations* (ODEs) in the variable x, with a complex parameter s.

$$u(x,s)_x = \mathcal{A}_s(x)u(x,s) \tag{16}$$

Remark 1 (Uniform flow): In the case of uniform flow, the flow variables are constant along the length of the channel, i.e., the discharge $Q_0(x) = Q_0 = Q_X$ and the stage $Y_0(x) = Y_n$ (normal depth).

A closed-form solution of the linearized Saint-venant equations in the uniform flow case can be obtained, relating the flow variables at any point x of the river reach $u(x,s)$ to the boundary conditions $u_1(0,s)$ and $u_2(X,s)$ (referring to [22] for details).

$$\begin{pmatrix} u_1(x,s) \\ u_2(x,s) \end{pmatrix} = \begin{pmatrix} g_{11}^u(x,X,s) & g_{12}^u(x,X,s) \\ g_{21}^u(x,X,s) & g_{22}^u(x,X,s) \end{pmatrix}\begin{pmatrix} u_1(0,s) \\ u_2(X,s) \end{pmatrix} \tag{17}$$

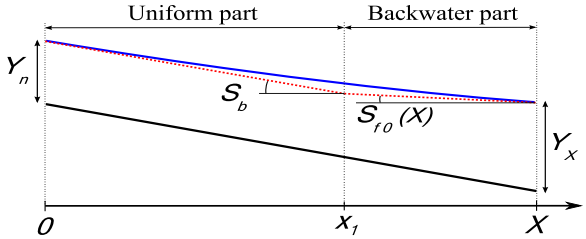

Fig. 1. *Backwater curve approximation*

where,

$$g^u_{11}(x,X,s) = \frac{\lambda_2 e^{\lambda_1 x+\lambda_2 X} - \lambda_1 e^{\lambda_2 x+\lambda_1 X}}{\lambda_2 e^{\lambda_2 X} - \lambda_1 e^{\lambda_1 X}}$$
$$g^u_{12}(x,X,s) = T_0 s \; \frac{e^{\lambda_1 x} - e^{\lambda_2 x}}{\lambda_2 e^{\lambda_2 X} - \lambda_1 e^{\lambda_1 X}}$$
$$g^u_{21}(x,X,s) = \frac{\lambda_1\lambda_2}{T_0 s} \; \frac{e^{\lambda_2 x+\lambda_1 X} - e^{\lambda_1 x+\lambda_2 X}}{\lambda_2 e^{\lambda_2 X} - \lambda_1 e^{\lambda_1 X}}$$
$$g^u_{22}(x,X,s) = \frac{\lambda_2 e^{\lambda_2 x} - \lambda_1 e^{\lambda_1 x}}{\lambda_2 e^{\lambda_2 X} - \lambda_1 e^{\lambda_1 X}}$$

Here, λ_1 and λ_2 are the eigenvalues of the ODE system (16), and are given by:

$$\lambda_i(s) = \frac{2T_0V_0 s + \gamma_0}{2\alpha_0} + (-1)^i \frac{\sqrt{4C_0^2T_0^2s^2 + 4T_0(V_0\gamma_0 - \alpha_0\beta_0)s + \gamma_0^2}}{2\alpha_0} \quad (18)$$

In the following sections, the transfer matrix for the uniform case is denoted as $\mathcal{G}^u(x,X,s) = (g^u_{ij}(x,X,s))$.

D. Transfer matrix for backwater approximation in non-uniform flow

For realistic cases, the backwater approximation is assumed to study flow regimes, in which the water elevation is not constant along the reach [11]. Following the method in [11], and further modified in [12], the backwater curve defined by equation (5) is approximated by two straight lines, as shown in Figure (1).

The river reach is then decomposed into two parts: a uniform part and a backwater part. The intersection of the two parts is denoted by x_1. Let x_u denote the location in the uniform part, $x_b = x - x_1$ denote the location in the backwater part, $X_u = x_1$ denote the length of the uniform part, and $X_b = X - x_1$ denote the length of the backwater part. $\mathcal{G}^b(x_b, X_b, s)$ denotes as the transfer matrices for the backwater parts, which has the same form as the transfer matrix in the uniform case $\mathcal{G}^u(x_u, X_u, s)$. The transfer matrix for the non-uniform case compromises the transfer matrices in both uniform and backwater parts and is denoted as $\mathcal{G}^n(x,X,s) = (g^n_{ij}(x,X,s))$:

$$\begin{pmatrix} u_1(x,s) \\ u_2(x,s) \end{pmatrix} = \begin{pmatrix} g^n_{11}(x,X,s) & g^n_{12}(x,X,s) \\ g^n_{21}(x,X,s) & g^n_{22}(x,X,s) \end{pmatrix} \begin{pmatrix} u_1(0,s) \\ u_2(X,s) \end{pmatrix} \quad (19)$$

E. Transfer matrix model for channel networks

The previous model (19) can be readily applied to channel networks. For simplicity, we consider a channel network

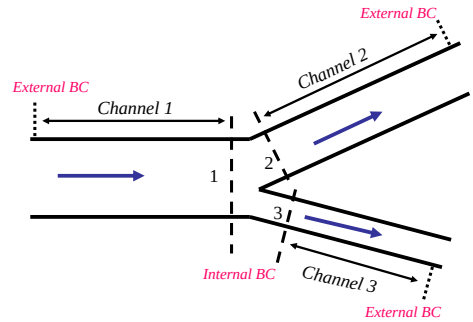

Fig. 2. *Representation of basic strategy for channel network.*

comprising three channels, as presented in Figure 2. Channel 1 is the upstream channel; Channels 2 and 3 are the downstream channels.

In each channel i ($i = 1,2,3$), $u_i(x,s)$ is defined as the two-dimensional flow vector in frequency domain, and X_i denotes the length of channel i:

$$u_i(x,s) = \begin{pmatrix} u_{i,1}(x,s) \\ u_{i,2}(x,s) \end{pmatrix} := \begin{pmatrix} q_i(x,s) \\ y_i(x,s) \end{pmatrix}, x \in [0, X_i] \quad (20)$$

The linear model (19) is applied to each branch in the channel network, and flow compatibility is examined at every interior junction.

$$\begin{pmatrix} u_{i,1}(X_i,s) \\ u_{i,2}(0,s) \end{pmatrix} = \begin{pmatrix} g^n_{i,11}(X_i,X_i,s) & g^n_{i,12}(X_i,X_i,s) \\ g^n_{i,21}(0,X_i,s) & g^n_{i,22}(0,X_i,s) \end{pmatrix} \begin{pmatrix} u_{i,1}(0,s) \\ u_{i,2}(X_i,s) \end{pmatrix} \quad i = 1,2,3$$
$$u_{1,2}(X_1,s) = u_{2,2}(0,s) = u_{3,2}(0,s)$$
$$u_{1,1}(X_1,s) = u_{2,1}(0,s) + u_{3,1}(0,s) \quad (21)$$

Given the external boundary conditions:

$$u_{1,1}(0,s), \quad u_{2,2}(X_2,s), \quad u_{3,2}(X_3,s) \quad (22)$$

all the other flow variables in the system (21) can be uniquely determined . The system is determinant.

Alternately, the system (21) can be expressed as:

$$Y = \mathcal{H}X \quad (23)$$

where vector X comprises of all the given external boundary conditions; vector Y contains all the undetermined external boundary conditions, concatenated with the internal boundary conditions:

$$\begin{aligned} X =& (u_{1,1}(0,s), u_{2,2}(X_2,s), u_{3,2}(X_3,s))^T \\ Y =& (u_{1,2}(0,s), u_{1,2}(X_1,s), u_{1,1}(X_1,s), \\ & u_{2,2}(0,s), u_{2,1}(0,s), u_{2,1}(X_2,s), \\ & u_{3,2}(0,s), u_{3,1}(0,s), u_{3,1}(X_3,s))^T \end{aligned}$$

The matrix $\mathcal{H}$ is a 9×3 matrix. The non-trivial element $g^n_{i,jk}$ (while $i = 1,2,3$, $j = 1,2$, $k = 1,2$) is a function of the *parameter vector* (Θ) of the system, which is defined as:

$$\Theta := (T_{0,i}, S_{b,i}, n, Q_{0,i}, Y_{0,i}(X))^T, \quad i = 1,2,3 \quad (24)$$

For each channel i, $Q_{0,i}$ is average discharge, $Y_{0,i}(X)$ is average depth, $T_{0,i}$ is average width, $S_{b,i}$ is bed slope, and n is the corresponding manning coefficient.
This method can be extended to more complex networks.

F. Model calibration

Before we use this model, the principal procedure for model calibration are model parameter adjustment and data reconciliation. The first step identifis the qualify parameter set; the second step removes measurments errors.

1) Parameter adjustment: The *parameter vector* Θ as defined in equation (24) has to be adjusted carefully to characterize the system.
In this study, the measurable parameters $Q_{0,i}$ and $Y_{0,i}(X)$ are evaluated based on the measurements at the stations, the bathymetry parameters $T_{0,i}$ and $S_{b,i}$ are derived from the geometry of the experiment field. The Manning coefficient n is optimized to let the the model output consistent with the measurement, following the method in [7].

2) Data reconciliation: Since the uncertainty in the input data would introduce errors in the model output, data reconciliation is applied to achieve the reconciliated boundary conditions, which are close to the measurements, and satisfy the Linearized Saint-Venant model.
The objective of the optimization problem is to minimize the total difference between measured flow vector M_{obv} and balanced flow vector $\tilde{M}$, which are weighted by the variance of the measurements W using the least square method. This can be expressed as:

$$f = (\tilde{M} - M_{\text{obv}})^T [diag(W)]^{-1} (\tilde{M} - M_{\text{obv}}) \tag{25}$$

One of the main advantages of our model decomposition is to transform a dynamic constraint into a static one in the frequency domain, which is easier to solve.
Rewrite the static model $Y = \mathcal{H}X$ in the following form:

$$\mathcal{C}\ M = 0 \tag{26}$$

with

$$M = \begin{pmatrix} X \\ Y \end{pmatrix}, \qquad \mathcal{C} = \begin{pmatrix} \mathcal{H} & -\mathrm{I} \end{pmatrix} \tag{27}$$

Here, I is an *Identity Matrix* with the same dimension as $\mathcal{H}$. This reconciliation problem now becomes a least square problem with static constraints. It reads:

$$\begin{aligned} \textbf{min} \quad & f = (\tilde{M} - M_{\text{obv}})^T [diag(W)]^{-1} (\tilde{M} - M_{\text{obv}}) \\ \textbf{s.t.} \quad & \mathcal{C}\ \tilde{M} = 0 \end{aligned} \tag{28}$$

We use the method suggested by [23] to solve the above data reconciliation problem. This constrained optimization problem can be further transferred into an unconstrained optimization problem using the Lagrange multiplier [24]:

$$L(\tilde{M}, \lambda) = (\tilde{M} - M_{\text{obv}})^T [diag(W)]^{-1} (\tilde{M} - M_{\text{obv}}) + 2\lambda\ \mathcal{C}\ \tilde{M} \tag{29}$$

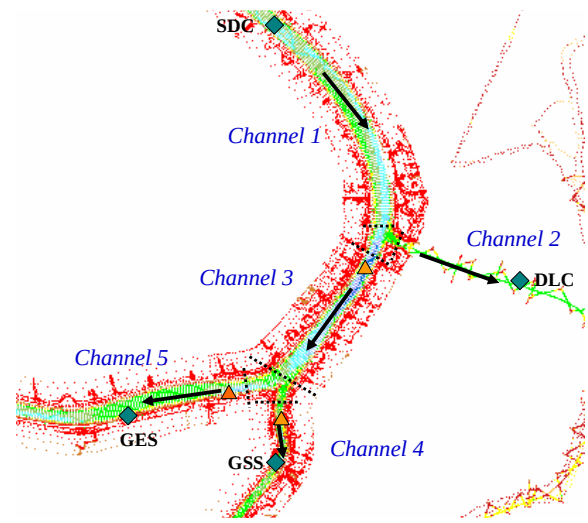

Fig. 3. *Experiment field at Sacramento River and Georgiana Slough.*

In order to obtain the unknown variables, the partially deviations are calculated and set to zero:

$$\begin{aligned} \frac{\partial L}{\partial \tilde{M}} &= 2(\tilde{M} - M_{\text{obv}})^T [diag(W)]^{-1} + 2\lambda\ \mathcal{C} = 0 \\ \frac{\partial L}{\partial \lambda} &= 2\lambda\ \mathcal{C}\ \tilde{M} = 0 \end{aligned} \tag{30}$$

This system of equations can be expressed in the matrix form using Gauss-Jordan method:

$$\begin{pmatrix} [diag(W)]^{-1} & \mathcal{C}^T \\ \mathcal{C} & \mathbf{0} \end{pmatrix} \begin{pmatrix} \tilde{M} \\ \lambda \end{pmatrix} = \begin{pmatrix} [diag(W)]^{-1} M_{\text{obv}} \\ \mathbf{0} \end{pmatrix} \tag{31}$$

Thus,

$$\tilde{M} = \begin{pmatrix} \mathbf{I} & \mathbf{0} \\ \mathbf{0} & \mathbf{0} \end{pmatrix} \begin{pmatrix} [diag(W)]^{-1} & \mathcal{C}^T \\ \mathcal{C} & \mathbf{0} \end{pmatrix}^{-1} \begin{pmatrix} [diag(W)]^{-1} M_{\text{obv}} \\ \mathbf{0} \end{pmatrix} \tag{32}$$

where, matrics $\mathbf{I}$ and $\mathbf{0}$ have the same dimension as $\mathcal{C}$.
With the reconciliated boundary condition $\tilde{X} = (\mathbf{I}\ \ \mathbf{0})^T \tilde{M}$, this model is ready to simulate the flow in the network system.

III. Case Study in Sacramento Delta

A. Field measurements

The Sacramento-San Joaquin Delta in California, is a valuable resource and an integral part of California's water system. This complex network covers 738,000 acres interlaced with over 1150 km of tidally-influenced channels and sloughs. The area of interest for our experiment is around the junction of Sacramento River and Georgiana Slough, as shown in Figure 3. The direction of mean river flow is specified with arrows; during tidal inversion the water would flow opposite way.

Four USGS stations, namely SDC, DLC, GES, and GSS, are located at the external boundary of this experiment field. The stations are marked as blue squares in Figure 3. Both discharge and stage were measured every 900 second at these

stations. The field data was collected between 10/23/2007 and 11/13/2007.

The following assumptions were made in this study:

- the flow is one dimensional;
- the channel geometry is fixed since the effects of sediment deposition and scour are negligible in the experiment period;
- the channel geometry can be modeled by a rectangular cross-section;
- the lateral and vertical accelerations are negligible;
- the pressure distribution is hydrostatic;
- there is no big jump along the channel, and the bed slope is smooth and small;
- the water surface across any cross-section is horizontal;

The input variables are the discharge perturbation at SDC ($u_{1,1}(X_1,t)$), the stage perturbation at DLC ($u_{2,2}(X_2,t)$), GSS ($u_{4,2}(X_4,t)$) and GES ($u_{5,2}(X_5,t)$). The output variables are the other four external boundary conditions, which are stage perturbation at SDC ($u_{1,2}(X_1,t)$), discharge perturbation at DLC ($u_{2,1}(X_2,t)$), GSS ($u_{4,1}(X_4,t)$) and GES ($u_{5,1}(X_5,t)$), as well as other flow variables within the channel network.

The parameters in this model are the average free surface width T_{0i}, the average bottom slope S_{bi}, the average Manning's coefficient n, the average discharge at upstream Q_{0i}, and the average downstream stage Y_{Xi} of channel i ($i = 1,2,3$). The data at three intermediate locations in the field is chosen to validate the model (marked in orange triangles).

B. Spectral analysis

The fundamental idea behind the model (19) is to decompose the input variables $u_{1,1}(0,t)$, $u_{2,2}(X_2,t)$, $u_{4,2}(X_4,t)$ and $u_{5,2}(X_5,t)$ into a finite sum of N dominant oscillatory modes. In the case of a channel network influenced by the ocean at the downstream end, these modes can be thought as the principle modes produced by the tidal forcing. The input variables are therefore expressed as:

$$u_{1,1}(0,t) \approxeq \sum_{k=0}^{N} \left[d_k^{(1,1,0)} e^{j\omega_k t} + \overline{d_k^{(1,1,0)}} e^{-j\omega_k t} \right] \tag{33}$$

$$u_{2,2}(X_2,t) \approxeq \sum_{k=0}^{N} \left[d_k^{(2,2,X_2)} e^{j\omega_k t} + \overline{d_k^{(2,2,X_2)}} e^{-j\omega_k t} \right] \tag{34}$$

$$u_{4,2}(X_4,t) \approxeq \sum_{k=0}^{N} \left[d_k^{(4,2,X_4)} e^{j\omega_k t} + \overline{d_k^{(4,2,X_4)}} e^{-j\omega_k t} \right] \tag{35}$$

$$u_{5,2}(X_5,t) \approxeq \sum_{k=0}^{N} \left[d_k^{(5,2,X_5)} e^{j\omega_k t} + \overline{d_k^{(5,2,X_5)}} e^{-j\omega_k t} \right] \tag{36}$$

with $d_k^{(1,1,0)}$, $d_k^{(2,2,X_2)}$, $d_k^{(4,2,X_4)}$ and $d_k^{(5,2,X_5)}$, $k = 0,\ldots,N$, are respectively the Fourier coefficients of the spectral decomposition of $u_{1,1}(0,t)$, $u_{2,2}(X_2,t)$, $u_{4,2}(X_4,t)$ and $u_{5,2}(X_5,t)$. ω_k is the set of frequencies used for the modal decomposition.

Figure 4 shows the spectral analysis for the discharge data at station SDC: There are three dominant tidal frequencies in

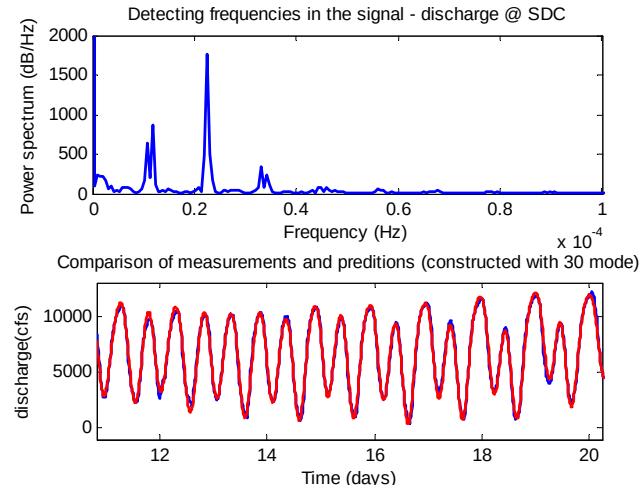

Fig. 4. *Spectrum analysis of discharge at SDC Station*

the system: $\omega_1 = 0.0001407\ s^{-1}$ (or period 12.4 hrs tide, corresponding to the M2 tide generated by the Moon), $\omega_2 = 0.0000727\ s^{-1}$ (or period 24 hrs tide, corresponding to the K1 tide generated by the Sun) and a $\omega_3 = 0.000068\ s^{-1}$ (or period 25 hrs tide). The power spectrum is cut-off at $70dB/Hz$ to determine the 30 dominant frequencies. The second plot in Figure 4 indicates that 30 modes are sufficient to capture the signal. The amplitude at 0 Hz is essentially the nominal stage. Similar arguments hold for other measurements.

C. Transfer matrix for channel network system

This open-channel network system has five simple channels as shown in Figure 3. Four given external boundary conditions are: the discharge at *SDC*: $u_{1,1}(X_1,s)$, the stage at *DLC*: $u_{2,2}(X_2,s)$, stage at *GSS*: $u_{4,2}(X_4,s)$, and stage at *GES*.

Following the method described in Section II-E, the network system can be expressed as:

$$Y = \mathcal{P}^{-1}\mathcal{Q}X \tag{37}$$

where,

$$X = (u_{1,1}(0,s), u_{2,2}(X_2,s), u_{4,2}(X_4,s), u_{5,2}(X_5,s))^T$$

$$Y = \begin{pmatrix} u_{1,2}(0,s) \\ u_{2,1}(X_2,s) \\ u_{4,1}(X_4,s) \\ u_{5,1}(X_5,s) \\ u_{1,2}(X_1,s) \\ u_{1,1}(X_1,s) \\ u_{2,1}(0,s) \\ u_{3,2}(X_3,s) \\ u_{4,1}(0,s) \\ u_{5,1}(0,s) \end{pmatrix}, \quad \mathcal{Q} = \begin{pmatrix} g_{1,11}^n & 0 & 0 & 0 \\ g_{1,21}^n & 0 & 0 & 0 \\ 0 & g_{2,12}^n & 0 & 0 \\ 0 & g_{2,22}^n & 0 & 0 \\ 0 & 0 & 0 & 0 \\ 0 & 0 & 0 & 0 \\ 0 & 0 & g_{4,12}^n & 0 \\ 0 & 0 & g_{4,22}^n & 0 \\ 0 & 0 & 0 & g_{5,12}^n \\ 0 & 0 & 0 & g_{5,22}^n \end{pmatrix}$$

$$\mathcal{P} = \begin{pmatrix} 1 & 0 & 0 & 0 & -g^n_{1,12} & 0 & 0 & 0 & 0 & 0 \\ 0 & 0 & 0 & 0 & -g^n_{1,22} & 1 & 0 & 0 & 0 & 0 \\ 0 & 0 & 0 & 0 & 1 & 0 & -g^n_{2,11} & 0 & 0 & 0 \\ 0 & 1 & 0 & 0 & 0 & 0 & -g^n_{2,21} & 0 & 0 & 0 \\ 0 & 0 & 0 & 0 & -1 & g^n_{3,11} & -g^n_{3,11} & g^n_{3,12} & 0 & 0 \\ 0 & 0 & 0 & 0 & 0 & g^n_{3,21} & -g^n_{3,21} & g^n_{3,22} & -1 & -1 \\ 0 & 0 & 0 & 0 & 0 & 0 & 0 & 1 & -g^n_{4,11} & 0 \\ 0 & 0 & 1 & 0 & 0 & 0 & 0 & 0 & -g^n_{4,21} & 0 \\ 0 & 0 & 0 & 0 & 0 & 0 & 0 & 1 & 0 & -g^n_{5,11} \\ 0 & 0 & 0 & 1 & 0 & 0 & 0 & 0 & 0 & -g^n_{5,21} \end{pmatrix}$$

D. Adjustment of model parameters

In this study, the elements of the *parameter vector* are tabulated in Table I.

TABLE I

PARAMETERS FOR SACRAMENTO RIVER AND GEORGIANA SLOUGH

Channel	$Q_{0,i}$	$Y_{X,i}$	$T_{0,i}$	$S_{b,i}$	n
$i=1$	186.73m^{3}s^{-1}	5.61m	115m	-0.00004	0.0323m$^{-1/3}$s
$i=2$	83.89m^{3}s^{-1}	4.04m	110m	-0.00009	0.0323m$^{-1/3}$s
$i=3$	113.08m^{3}s^{-1}	7.74m	110m	-0.00004	0.0323m$^{-1/3}$s
$i=4$	58.07m^{3}s^{-1}	4.02m	56m	-0.00019	0.0323m$^{-1/3}$s
$i=5$	65.24m^{3}s^{-1}	5.27m	89m	-0.00004	0.0323m$^{-1/3}$s

The mean discharge ($Q_{0,1}$) of the channels 1,2,4,5 are calculated using the measured discharge at *SDC*, *DLC*, *GSS*, *GES* respectively. It is clear that the measurement data are inconsistent, since $Q_{0,1} \neq Q_{0,2} + Q_{0,4} + Q_{0,5}$. To partially compensate the measurement error, the mean discharge at channel 3 is set to be: $Q_{0,3} = [(Q_{0,1} - Q_{0,2}) + (Q_{0,4} + Q_{0,5})]/2$. The model outputs $u_{1,2}(0,s)$, $u_{2,1}(X_2,s)$, $u_{4,1}(X_4,s)$, and $u_{5,1}(X_5,s)$ are shown in Figure 5, along with the measurement data for comparison. It is observed that the model gives a good estimation in Sacramento river (*SDC* and *GES*) but performs poorly at *DLC* and *GSS*. This may be due to measurement error in the boundary conditions.

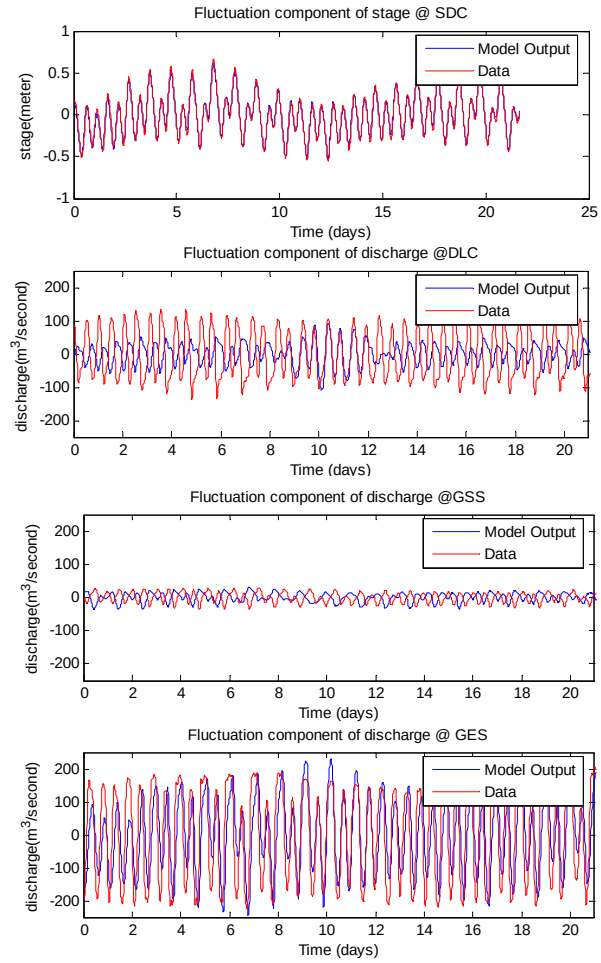

Fig. 5. *Comparison of model output and measurement data at external boundaries of the network.*

E. Boundary condition reconciliation

The method developed in Section II for the data reconciliation problem has been implemented to solve the reconciliated boundary conditions of this case. The static model (37) can be rewritten in the following form:

$$\mathcal{C}\ M = 0 \tag{38}$$

with

$$M := (u_{1,1}(0,s), u_{2,2}(X_2,s), u_{4,2}(X_4,s), u_{5,2}(X_5,s), u_{1,2}(0,s), u_{2,1}(X_2,s), u_{4,1}(X_4,s), u_{5,1}(X_5,s))^T \tag{39}$$

$$\mathcal{C} = [(\mathbf{I}^{4\times 4} \quad \mathbf{0}^{4\times 6})\mathcal{P}^{-1}\mathcal{Q} \quad -\mathbf{I}^{4\times 4}] \tag{40}$$

A least square problem similar to (28) is solved. The solution are shown in Figure 6 and 7. Clearly, the reconciliated data are very close to the measurements

F. Model validation

Flow variables at three locations are chosen from the network to further validate the model. The locations are marked as orange triangles in Figure 3, and data are collected between 11/01/2007 and 11/12/2007. Location A is at downstream of the junction of Sacramento river and Delta Cross channel; Location B is at downstream of GSS branch; Location C is at downstream of Sacramento Branch. The discharge at Location A, along with the stage data at three locations, are used to test the model. The simulation results are shown in Figure 8.

Model calibration and validation are further evaluated using standard statistical metrics. The primary evaluation measure is the coefficient of efficiency, E [25]:

$$E = 1 - \left[\frac{\sum_1^N (\hat{u}_i - u_i)^2}{\sum_1^N (u_i - \overline{u_i})^2}\right] \tag{41}$$

where $\hat{u}_i$ is the simulated flow (or other variables of interest), u_i is the observed flow, and $\overline{u_i}$ is the mean of u_i, for $i = 1\ to\ N$ measurement times (or events). If a model predicts observed variables perfectly, $E = 1$. If $E < 0$, the model's predictive power is worse than simply using the average of observed values.

Another statistic evaluation of the analysis is the correlation coefficient (λ), given by:

$$\lambda = \frac{\sum_1^N (u_i - \overline{u_i})(\hat{u}_i - \overline{\hat{u}_i})}{\sqrt{\sum_1^N (u_i - \overline{u_i})^2 \sum_1^N (\hat{u}_i - \overline{\hat{u}_i})^2}} \tag{42}$$

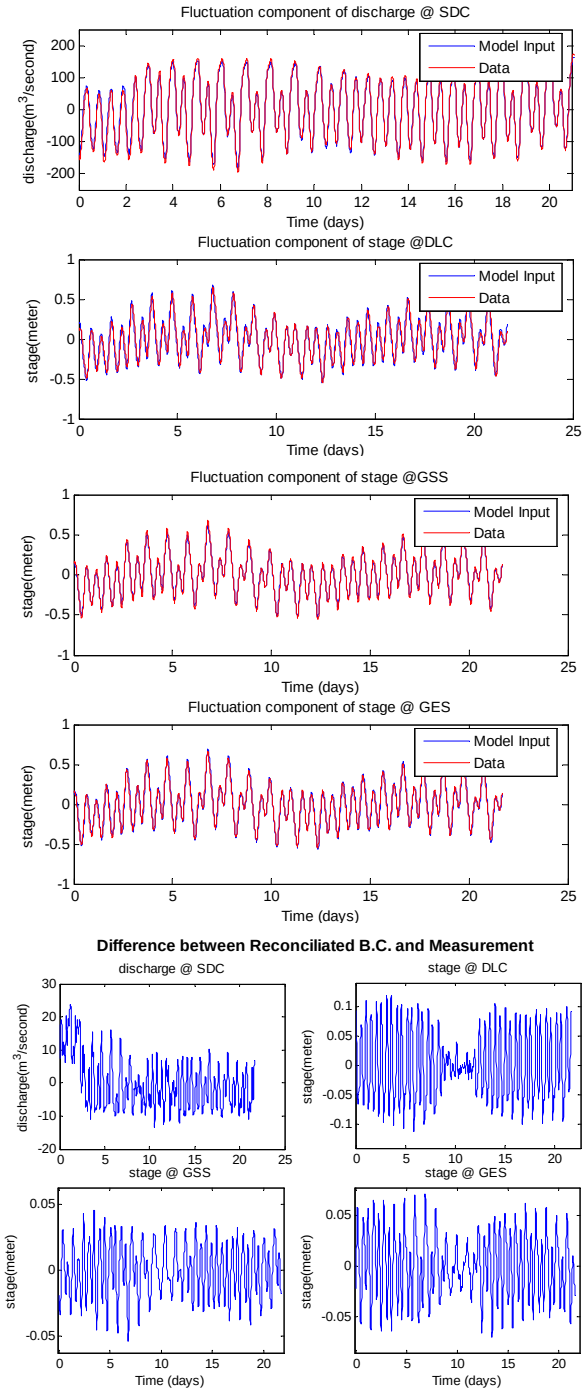

Fig. 6. *Reconciliated oundary condition v.s. measurement.*

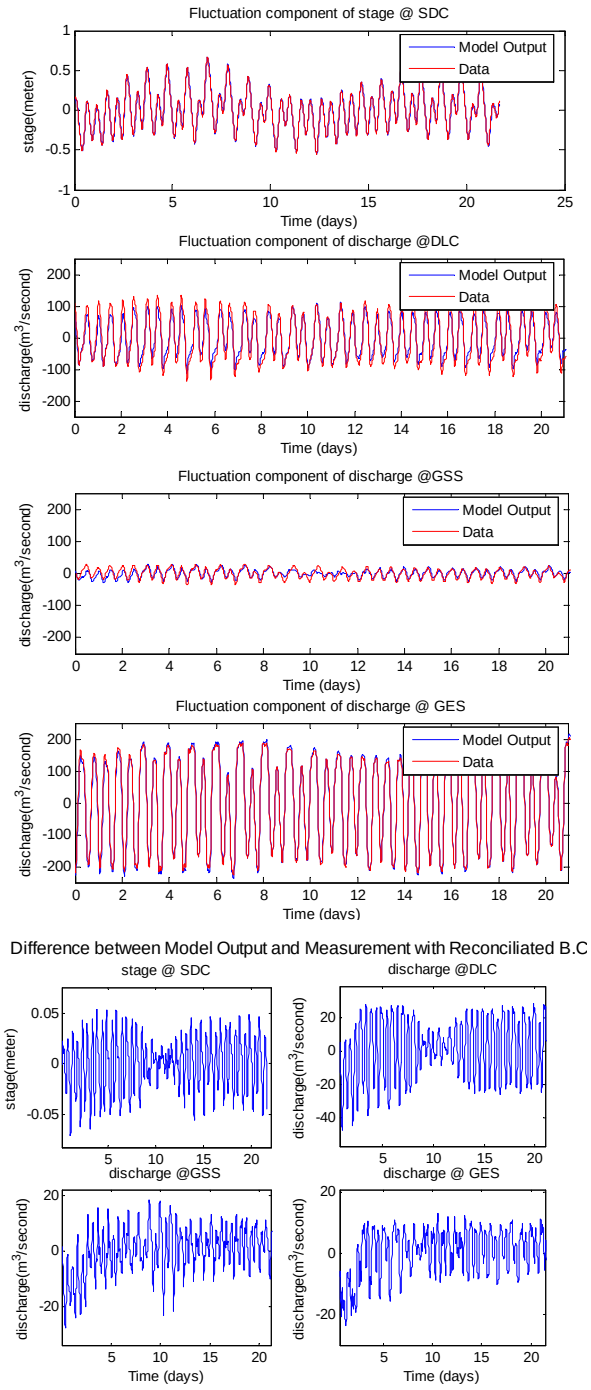

Fig. 7. *Model output using reconciliated boundary conditions v.s. measurement.*

where, $\overline{u_i}$ and $\overline{\hat{u}_i}$ represent the mean of measured and simulated flow for $i = 1$ *to* N measurement times, respectively. Table II enlists the values of λ and E in the validation sets.

TABLE II

λ-VALUE AND E-VALUE FOR MODEL VALIDATION

Location	A	A	B	C
Variables	discharge	stage	stage	stage
E	0.9775	0.9643	0.9768	0.9612
λ	0.9895	0.9876	0.9897	0.9875

Both λ-values and E-values are close to unity. The results in Table II and Figure 8 indicate that our model can accurately simulate the channel flow.

IV. Conclusion

This article proposes a new model to estimate the flow variables in a channel network system subjected to periodic forcing. A spatially-dependent channel network model in frequency domain is constructed using transfer

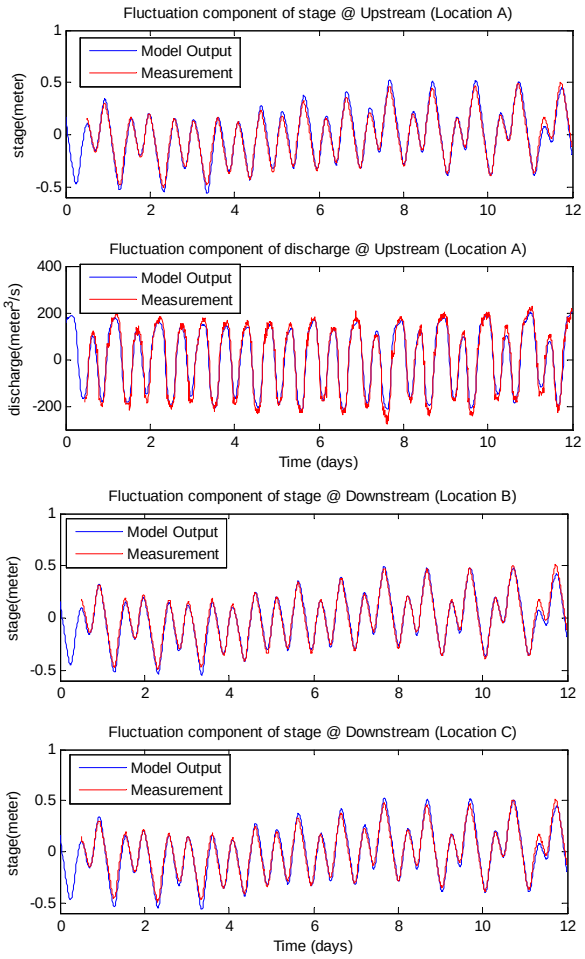

Fig. 8. *Validate the model output with measurement.*

matrix for the non-uniform steady state case. The model decomposition allows the output response to be expressed in terms of the spectral coefficients of the input variables and the transfer matrix coefficients evaluated at appropriate locations. Parameter adjustment and static data reconciliation efficiently select the desired parameter vector and remove the error of the measurement data. Subsequently, the flow properties at any location in the system can be readily predicted.

The approach proposed in this study has been successfully applied to a channel network in the Sacramento-San Joaquin Delta, with the flow prediction being successfully validated at three locations intermediate the channel system.

V. Acknowledgments

This article was written when Xavier Litrico was visiting scholar at UC Berkeley. Financial support of Cemagref is gratefully acknowledged. Real-time flow data at *USGS* stations are downloaded from the *California Data Exchange Center* (CDEC) of *Dept. of Water Resources* (DWR) (http://cdec.water.ca.gov). The flow data used for validation is provided by Prof. Mark Stacey, Julie Percelay and Maureen Downing-Kunz from UC Berkeley.

References

[1] *Enhanced Calibration and Validation of DSM2 HYDRO and QUAL*, California Department of Water Resources.

[2] *TELEMAC 2D. Version 5.2 – Principle note*, Report EDF, 2002.

[3] *Coastal and Inland Waters in 2D*, DHI Software, 2004.

[4] T. Molls and F. Molls, "Space-time conservation method applied to saint venant equations." *J. Hydr. Engrg.*, vol. 124, no. 5, pp. 501–508, 1998.

[5] R. Cooley and S. Moin, "Finite element solution of saint venant equations." *J. Hydraul. Div.*, vol. HY6, pp. 759–775, 1976.

[6] R. Szymkiewicz, "Finite-element method for the solution of the saint venant equations in an open channel network." *Journal of Hydrology*, vol. 122, no. 1-4, pp. 275–287, 1991.

[7] Q. Wu, S. Amin, S. Munier, A. Bayen, X. Litrico, and G. Belaud, "Parameter identification for the shallow water equations using modal decomposition," in *Proceedings of the 46th Conference of Decision and Control*, 2007.

[8] R. Gorriga, F. F. Patta, S. Sanna, and G. Usai, "A mathematical model for open channel networks." *Appl. Math. Mod.*, vol. 23, pp. 51–54, 1979.

[9] Y. Ermolin, "Study of open-channel dynamics as controlled process." *J. of Hydraulic Eng.*, vol. 119, no. 1, pp. 59–71, 1992.

[10] J. Baume and J. Sau, "Study of irrigation cannal dynamics for control purposes." in *Int. Work shop RIC'97*, Marrakech, Morroco, 1997.

[11] J. Schuurmans, A. J. Clemmens, S. Dijkstra, A. Hof, and R. Brouwer, "Modeling of irrigation and drainage canals for controller design," *J. Irrig. Drain. Eng.*, vol. 125, no. 6, pp. 338–344, 1999.

[12] X. Litrico and V. Fromion, "Simplified modeling of irrigation canals for controller design," *J. Irrig. Drain. Eng.*, vol. 130, no. 5, pp. 373–383, 2004.

[13] C. Reimers, J. Werther, and G. GruhnX, "Flowsheet simulation of solids processes data reconciliation and adjustment of model parameters," *Chemical Engineering and Processing*, vol. 47, p. 138¨C158, 2008.

[14] N. Bedjaoui, X. Litrico, A. Lourosa, and J. R. Bruno, "Application of data reconciliation on an irrigation canal." in *7th conference on Hydroinformatics*, vol. II, 2006, pp. 1503–1510,.

[15] C. M. Crowe, "Data reconciliation–progress and challenge," *Journal of Process Control*, vol. 6(2/3), pp. 89–98, 1996.

[16] M. Alhaj-Dibo, D. Maquin, and J. Ragot, "Data reconciliation: A robust approach using a contaminated distribution," *Control Engineering Practice*, vol. 16, p. 159¨C170, 2008.

[17] J. Deltour, E. Canivet, F. Sanfilippo, and J. Sau, "Data reconciliation on the complex hydraulic system of canal de provence," *J. Irrig. and Drain. Engrg.*, vol. 131, no. 3, pp. 291–297, 2005.

[18] M. J. Bagajewicz and E. Cabrera, "Data reconciliation in gas pipeline systems." *Ind. Eng. Chem. Res.*, vol. 42, no. 22, pp. 5596 –5606, 2003.

[19] J. Ragot and D. Maquin, "Reformulation of data reconciliation problem with unknown-but-bounded errors." *Industrial and Engineering Chemistry Research*, vol. 43, no. 6, pp. 1530–1536, 2004.

[20] V. Chow, *Open-channel Hydraulics*. McGraw-Hill Book Company.

[21] J. Cunge, F. Holly, and A. Verwey, *Practical aspects of computational river hydraulics*. Pitman, 1980.

[22] X. Litrico and V. Fromion, "Frequency modeling of open channel flow," *J. Hydraul. Eng.*, vol. 130, no. 8, pp. 806–815, 2004.

[23] G. Heyen, M. N. Dumont, and B. Kalitventzeff, "Computer-aided design of redundant sensor networks." *Comput. Chem. Eng.*, vol. 10, pp. 685–690, 2002.

[24] S. Boyd and L. Vandenberghe, *Convex Optimization*. Cambridge University Press.

[25] J. Nash and J. Sutcliffe, "River flow forecasting through conceptual models: part i. a discussion of principles." *Journal of Hydrology*, vol. 10, pp. 282–290, 1970.